



A new rockburst criterion of stress–strength ratio considering stress distribution of surrounding rock

Xiqi Liu¹ · Gang Wang^{1,2} · Leibo Song² · Guansheng Han² · Wenzhao Chen³ · Hao Chen²

Received: 5 September 2022 / Accepted: 9 December 2022 / Published online: 30 December 2022
© Springer-Verlag GmbH Germany, part of Springer Nature 2022

Abstract

Rockburst is a common geological disaster in the process of deep rock excavation, and stress gradient is an important factor affecting rockburst. In this paper, the concept of “stress concentration” was proposed. The relevant data of a large number of engineering rockburst cases were statistically analyzed, and a new rockburst criterion of stress–strength ratio considering stress gradient of surrounding rock was established. The research results revealed that the rockburst criterion considering the stress gradient distribution of surrounding rock could effectively overcome the problem of non-uniform division of rockburst criteria in the traditional strength-to-stress ratio. It can fully reflect the influence of tunnel size effect on rockburst. There was a significant correlation between rockburst strength and stress gradient, and different rockburst strengths showed obvious zoning concentration phenomenon on the two-dimensional plane. The established rockburst criterion considering the stress intensity ratio of surrounding rock had strong applicability, and the prediction accuracy could reach more than 90%. The proposed rockburst criterion in this paper has certain theoretical and engineering guiding value for the early warning of underground engineering disasters.

Keywords Strain rockburst · Stress–strength ratio · Stress gradient · Rockburst intensities · Rockburst prediction

Introduction

At the current time, with the increase of deep rock excavation in a high in situ stress environment, rockburst phenomenon has become a major geological engineering problem in deeply buried long tunnels. This has increasingly highlighted the need for effective rockburst prevention and control strategies (Li et al. 2017a; Taromi et al. 2017; Afraei et al. 2018; Rudziński et al. 2019; Oge and Cirak 2019; Kaiser and Moss 2022; Niu et al. 2022). The accurate predictions of rockburst can assist in taking appropriate engineering countermeasures in the designs and construction of engineering projects to

reduce or avoid losses caused by rockburst disasters (Guo et al. 2017; Feng et al. 2019; Forbes et al. 2020). At present, there are many research results available regarding rockburst phenomena. However, the various theoretical prediction methods based on rockburst theories and rockburst failure mechanisms still present difficulties in engineering applications (Hauquin et al. 2018; Wojtecki et al. 2022). Therefore, the study of rockburst mechanisms and prediction models is of great significance for guiding engineering practices.

In engineering practices, rockburst is generally predicted using simple stress grading methods. For example, the ratios of the tangential stress levels following excavation activities or the maximum principal stress levels of the far fields to the uniaxial compressive strength of the surrounding rock masses are used as the discriminant indexes. These rockburst criteria include the Tao, Barton, Norway, Russense, Hoek criteria, and so on (Zhao et al. 2016). However, since the current rockburst criteria based on strength theory do not include the comprehensive influences of various important factors, the gaps between the calculated results and the actual results are relatively large. Therefore, nonlinear theories have been introduced to predict rockburst, such as genetic algorithm methods and Bayesian evaluation methods

✉ Gang Wang
2021000077@usx.edu.cn

¹ Key Laboratory of Geotechnical and Structural Engineering Safety of Hubei Province, School of Civil Engineering, Wuhan University, Wuhan 430070, China

² School of Civil Engineering, Shaoxing University, Shaoxing 312000, China

³ School of Civil Engineering, University of South China, Hengyang 421001, China

(Li et al. 2017b, c; Dong et al. 2016). However, it has been found that due to the minimal amount of in-depth exploration which has been conducted regarding the relationships between the various influencing factors, and the necessity for setting the weights of the main factors and each discriminant factor, it has proven difficult to fully reflect the degrees of dependence or interdependence of the influencing factors. Therefore, the applications of the previously mentioned distinguished methods thus far have been limited. Currently, although the neural network method, support vector machine method, and distance discrimination method have solved the problems mentioned above (Zhou et al. 2012; Diederichs 2018), there have been further limitations caused by “bottleneck” problems when acquiring knowledge, and the existing limitations have negatively affected the potential for its engineering applications.

The strain rockburst mainly occurs during the loading process of the tangential stress concentration after the tunnel excavation. Therefore, regardless of whether it is a single-factor rockburst criterion or multi-factor nonlinear prediction method, the rockburst criteria based on strength theory are often used as the key indicators in predicting strain rockburst conditions (Li et al. 2017d; Kong et al. 2019). The rockburst criteria based on the strength theory are mainly from the relationship between the strength of the rock masses and the concentrated secondary stress of the surrounding rock masses. The relative magnitude of the stress is used as the failure criterion. However, the deformations of surrounding rock masses caused by excavation activities are dependent not only on the stress levels of the rock masses but also on the stress paths and their original stress histories (Xie et al. 2015). During the excavations of underground tunnels, the surrounding rock masses will experience complex stress paths. The tangentially concentrated stress of the tunnel remains more significant at the excavation boundary and presents a descending trend toward the interior of the surrounding rock masses with a specific gradient (Miao et al. 2016). Also, the excavation methods, tunnel sizes, and geological structure of the surrounding rock masses all impact stress distributions of surrounding rock. Liu et al. (2017) pointed out that the size effect exists in the rockburst intensity, which is mainly due to the change of energy storage depth and energy release caused by the stress distribution of surrounding rock. That is the nonlinear rule. The energy release rate tends to be strong with the increase of the diameter of the tunnel and then decreases with the increase of the diameter of the tunnel when it exceeds a specific diameter scale. Liu et al. (2021) and Huo et al. (2020) demonstrated that the rockburst intensity is related to the tangential stress gradient of surrounding rock through indoor rockburst model tests, and the rockburst intensity of the model increased with the increase of stress gradient. From this viewpoint, a strength criterion method that simply considered the stress

of the surrounding rock and ignored the stress path distribution may not be comprehensive to some degree in its results.

Therefore, based on the analysis of the influencing factors of rockburst phenomenon, the tangential stress distribution of surrounding rock is considered, and the concept of stress gradient is introduced. In addition, a quantitative representation of the surrounding rock stress gradient values is also provided. Based on engineering rockburst examples, the corresponding rockburst intensities were expressed in the two-dimensional plane determined by the stress–strength ratio and stress gradient. Then, through the empirically fitted expressions, a more accurate and reasonable rockburst criterion was established. The achieved results will provide new ideas and approaches for rockburst prediction in deep underground engineering.

Analysis of the main factors affecting the rockburst phenomena

The present study determined that to avoid rockbursts, the factors that affect rockburst need to be fully understood. Rockburst is a phenomenon resulting from rock mass failures. These failures are caused by the high-stress concentration conditions of the surrounding rock masses following tunnel excavation activities. It has been observed that although there are many inducing factors, regardless of how complicated the internal mechanisms are, the rockburst is mainly controlled by two factors: the rock mass conditions and the stress field conditions (Miao et al. 2016).

Rock mass conditions

As the intrinsic influencing factors of rockburst, the rock mass conditions mainly referred to the hard and brittle nature of surrounding rock mass (Wang et al. 2015). The “hard” nature of the surrounding rock masses is determined by the uniaxial compressive strength σ_{ci} and the rock integrity index K_v . Generally speaking, it has been found that the higher the uniaxial compressive strength and the more complete the rock masses, the more favorable the conditions for the rock masses to store strain energy. The “brittleness” of the surrounding rock masses is determined by the impact energy index $W_{et} = \Phi_{sp} / \Phi_{st}$, which is the ratio of the anterior peak area Φ_{sp} and the post-peak area Φ_{st} of the uniaxial compression stress–strain curve of the surrounding rock masses; and the brittleness coefficient $B = \sigma_{ci} / \sigma_t$, which is the ratio of the axial compression strength σ_{ci} to the uniaxial tensile strength σ_t . It is generally believed that the larger the W_{et} and B value, the higher the elastic energy release rate during rockburst failures, the more favorable the conditions for rockburst.

It has been previously observed that the greater the instantaneous release of energy from the surrounding rock masses in tunnel excavations, the greater the likelihood of rockburst. For this reason, the rockburst phenomena mainly occur in fresh and intact rock masses with hard textures and high structural densities, where there are no or few cracks, and the material tends to be hard and brittle.

Stress field conditions

As the external influencing factors of rockburst, the stress field conditions refer to the secondary stress fields of the surrounding rock masses following excavation activities. The stress field conditions generally refer to the tangential stress of the surrounding rock, subject to an initial in situ stress state and such engineering excavation conditions such as engineering layouts, excavation forms, and excavation methods dependent on the mechanical properties of the rock masses (Guo et al. 2017).

At present, the stress field conditions for rockburst are usually expressed by the ratio of the maximum tangential stress or the maximum principal stress around the surrounding rock masses to the uniaxial compressive strength of surrounding rock. When a tunnel is excavated, the initial stress state of the original rock will be disturbed, and the initial stress balance of the surrounding rock masses will be destroyed, which results in stress redistributions. It is known that the high concentrations of the secondary stress cause the stress of surrounding rock masses to exceed the critical stress generated by the rockburst, thereby resulting in the occurrences of rockburst phenomena. Therefore, the stress–strength ratios of the surrounding rock, as the core factors controlling the rockburst, are often used as critical indicators for rockburst predictions. The rockburst criteria based on strength theory commonly used for hard and brittle rock masses are shown in Table 1.

As can be seen in Table 1, there are two leading indicators in the rockburst criteria. One is the uniaxial compressive strength of the surrounding rock masses, and the other is the

stress level in the surrounding rock masses of the tunnels. At present, the most widely used indicator is the ratio of the maximum tangential stress $\sigma_{\theta_{max}}$ of the surrounding rock to the uniaxial compressive strength σ_{ci} of the rock. However, a major current controversy exists regarding the critical value of the criteria, and the accuracy of the rockburst predictions has been relatively lower.

The gradient distributions of the tangential stress of the surrounding rock masses

The failure modes of rockburst are determined by the rock mass types and the stress states of the surrounding rock masses. Among the known affecting factors of rockburst, the methods used to assess the lithology conditions of rock masses are relatively comprehensive. The main factors influencing the formation, expansion, and fusion of surrounding rock fissures include the following two points: (1) the principal stress magnitude; (2) the principal stress direction (as shown in Fig. 1). However, the most commonly used criterion-based strength theory mainly reflects the influence of principal stress magnitude on the rockburst intensity when considering the stress field conditions affecting rockburst.

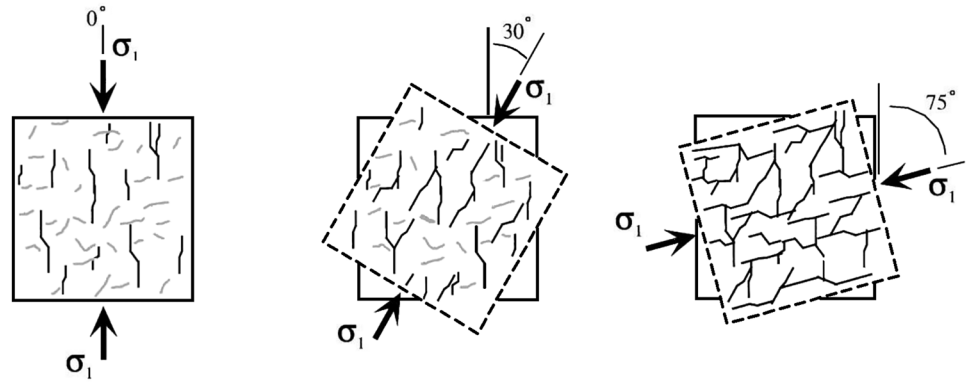
The directions of extension of cracks in rock masses are affected by the rotation of the principal stress axis. The generation, expansion, and penetration of secondary fractures in rock masses occur along the direction of the maximum principal stress or form small angles with the maximum principal stress direction (Luo et al. 2020; Song et al. 2022). Due to the underground openings, the tangentially concentrated stress of the tunnel remains larger at excavation boundary and decreases toward the interior of the surrounding rock with a certain gradient. The tangential stress of this gradient distribution subsequently leads to varying degrees of deflection of the principal stress direction, thereby affecting the deformations and failure mechanisms of the surrounding rock masses. As shown in Fig. 2, Liu et al. (2021) used the simplified formula of surrounding rock tangential stress distribution to express the gradient distribution of surrounding

Table 1 Rockburst criteria based on strength theory (Zhou et al. 2012)

Criterion	Regional engineering	Discriminant	Intensity grading			
			No	Light	Medium	Violent
Russense	Norwegian Mine	$\sigma_{\theta_{max}}/\sigma_{ci}$	<0.2	0.2 to 0.3	0.3 to 0.55	≥ 0.55
Turchaninov	Kola Peninsula Mine	$(\sigma_{\theta_{max}} + \sigma_L)/\sigma_{ci}$	≤ 0.3	0.3 to 0.5	0.5 to 0.8	≥ 0.8
Tao	Chinese Tunnel	σ_{ci}/σ_1	> 14.5	5.5 to 14.5	2.5 to 5.5	≤ 2.5
Hoek	South African Mine	$\sigma_{\theta_{max}}/\sigma_{ci}$	<0.34	<0.42	<0.56	>0.7
Xu	Erlang Mountain	$\sigma_{\theta_{max}}/\sigma_{ci}$	<0.3	0.3 to 0.5	0.5 to 0.7	>0.7

In the table, σ_{ci} is the uniaxial compressive strength (MPa) of rock; $\sigma_{\theta_{max}}$ is the maximum tangential stress (MPa) in the section of underground space; σ_1 represents the maximum principal stress (MPa) in the ground stress tensor; and σ_L denotes the axial stress (MPa) along the direction of the excavation in underground space

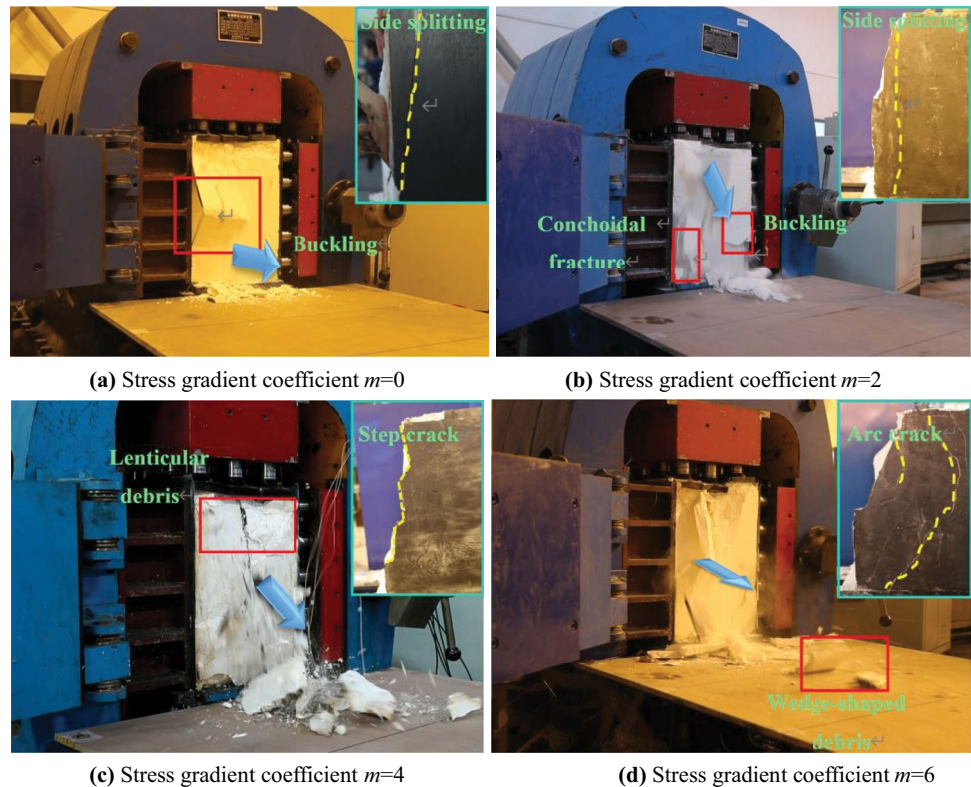
Fig. 1 Effects of the principal stress direction on fracture development (Eberhard 2001)



rock tangential stress, quantified the stress gradient coefficient by m ($m \geq 0$) value (the larger m , the greater the loading stress gradient), and analyzed the rockburst phenomenon under different stress gradient loading conditions through laboratory tests. It is found that, within a certain stress gradient, with the increase of the loading stress gradient, the rockburst intensity increases and the failure stress decreases, and the main failure of the model is transitioned from tensile failure to shear failure. It shows that the stress gradient has a significant influence on the evolution process of rockburst.

However, in the stress field conditions of the current rockburst criteria, the rockbursts are judged only in the one dimension of the strength theory, which is essentially not comprehensive to some degree. Therefore, under stress field conditions, by considering the influences of the stress magnitudes and stress distributions on the rockburst, the conditions will be more consistent with the stress of surrounding rock masses evolution processes of the tunnel walls. It can then be concluded that considering the stress distribution index can help establish a more reasonable rockburst criterion for rockburst phenomena predictions.

Fig. 2 Rockburst moment of the model under different gradients (Liu et al. 2021)



Rockburst criterion of SR-SG

The above analysis shows that the stress intensity ratio and the tangential stress distribution of surrounding rock have influence on the intensity and failure stress of rockburst. In order to consider the influence of the stress intensity ratio and the tangential stress distribution of surrounding rock on rockburst in the engineering, a new rockburst criterion of stress–strength ratio considering stress gradient of surrounding rock (SR-SG) is established on the basis of the quantitative expression of the stress gradient.

Quantitative expression of stress gradient

As shown in Fig. 3, it has been observed that the tangentially concentrated stress of the tunnel remained larger at the excavation boundary, presented a descending trend toward the interior of the surrounding rock masses, and tended to the original rock stress value eventually. It is necessary to simplify the surrounding rock mass’s stress in the disturbance zone to quantify the distribution of tangential stress gradient in surrounding rock.

As shown in Fig. 3, it is assumed that the vertical stress and horizontal stress of the excavated rock mass are σ_1 and σ_3 , the diameter of tunnel radius is a , the lateral pressure coefficient $\lambda = \sigma_3/\sigma_1$, and x is the radial distance (m) from a point in the surrounding rock to the tunnel center. When the lateral pressure coefficient $\lambda \leq 1$, the failure is mainly concentrated on the two sides of the tunnel. Therefore, the tangential stress distribution of the surrounding rock with $\theta = 0^\circ$ is discussed.

The tangential stress σ_θ and radial stress σ_r of the surrounding rock with $\theta = 0^\circ$ are (Yu and Wang 2021):

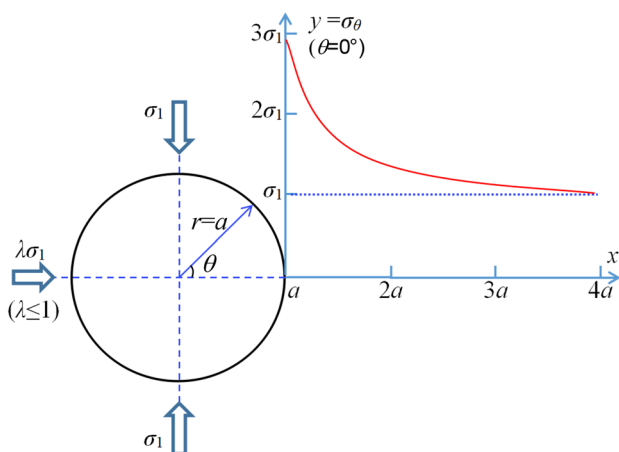


Fig. 3 Tangential stress distributions of the surrounding rock masses in a deeply buried tunnel

$$\sigma_\theta = \frac{1}{2}\sigma_1(1 + \lambda)(1 + \frac{a^2}{x^2}) + \frac{1}{2}\sigma_1(1 - \lambda)(1 + \frac{3a^4}{x^4}) \quad (1)$$

$$\sigma_r = \frac{1}{2}\sigma_1(1 + \lambda)(1 - \frac{a^2}{x^2}) - \frac{1}{2}\sigma_1(1 - \lambda)(1 + \frac{3a^4}{x^4} - \frac{4a^2}{x^2}) \quad (2)$$

Excavation disturbance stress is:

$$\sigma_\theta - \sigma_1 = \frac{\sigma_1 a^2 (1 + \lambda)}{2x^2} + \frac{3\sigma_1 a^4 (1 - \lambda)}{2x^4} \quad (3)$$

$$\sigma_r - \sigma_3 = -\frac{\sigma_1 a^2 (5\lambda - 3)}{2x^2} - \frac{3\sigma_1 a^4 (1 - \lambda)}{2x^4} \quad (4)$$

Then the rate of change of disturbance stress with x is:

$$\frac{d(\sigma_\theta - \sigma_1)}{dx} = \frac{-\sigma_1 a^2 (1 + \lambda)}{x^3} + \frac{-6\sigma_1 a^4 (1 - \lambda)}{x^5} \quad (5)$$

$$\frac{d(\sigma_r - \sigma_3)}{dx} = \frac{\sigma_1 a^2 (5\lambda - 3)}{x^3} + \frac{6\sigma_1 a^4 (1 - \lambda)}{x^5} \quad (6)$$

By the Eq. (5), the surrounding rock excavation disturbing tangential force rate of change gradually decreases with the increase of x . Because the rockburst generally occurs near the tunnel wall, the absolute value of the stress change rate of the surrounding rock at the tunnel wall can be used to represent the stress gradient value of the surrounding rock. Subtract $x = a$ into Eqs. (5) and (6) to obtain the tangential stress gradient coefficient (TSGC) and radial stress gradient coefficient (RSGC) of surrounding rock:

$$TSGC = \frac{\sigma_1}{a}(7 - 5\lambda) \quad (7)$$

$$RSGC = \frac{\sigma_1}{a}(3 - \lambda) \quad (8)$$

Equations (7) and (8) indicate that TSGC and RSGC are both in direct proportion to σ_1 and inversely proportional to a , and the change rule of both is consistent.

Statistical analysis of cases

As the leading cause of surrounding rock failure is the compression process of tangential stress concentration, the tangential stress gradient coefficient TSGC is taken as the indicator to distinguish rockburst in this paper. In this study, based on the current related research results and in situ rockburst data (Zhou et al. 2012; Feng et al. 2019), a total of 81 rockburst instances were examined, as shown in Table 2. The corresponding values of TSGC and the stress–strength ratio R ($R = \sigma_{\theta_{max}}/\sigma_{ci}$) (Zhou et al. 2012) were calculated using the engineering measured data. The corresponding rockburst

Table 2 Engineering rockburst cases (Billington et al. 2011; Zhou et al. 2012; Feng et al. 2019)

Tunnel name	Tunnel diameter D_0 /m	σ_{ci} /MPa	σ_1 /MPa	$\sigma_{\theta max}$ /MPa	$\sigma_{\theta max}/\sigma_{ci}$	$TSGC/MPa \cdot m^{-1}$	Rockburst level
Mine-by Test Hole	3.5	220	60	169	0.77	293.7381	Light
Jinping II Tunnel	13	140	70	114.8	0.82	51.76615	Medium
Jinping II Tunnel	7.2	120	48	98.6	0.82	57.0212	Violent
Neelum-Jhelum Diversion Tunnel	11.7	132.64	64.80–77.76	238.7520	1.80	212.67747	Violent
		136.26	65.61–78.73	239.8176	1.76	210.63529	Violent
		138.53	66.42–79.70	239.6569	1.73	196.17742	Violent
		130.79	67.23–80.68	239.3457	1.83	200.48809	Violent
		128.45	68.04–81.68	238.9170	1.86	195.15841	Violent
		131.17	61.9–74.36	238.7294	1.82	230.2305	Violent
		130.31	62.69–75.23	239.7704	1.84	227.956	Violent
		136.46	50.03–60.03	121.4494	0.89	92.95009	Medium
		141.58	50.21–60.26	120.3430	0.85	90.978	Medium
		141.67	50.40–60.48	120.4195	0.85	90.61786	Medium
		137.91	50.58–60.70	121.3608	0.88	91.45779	Medium
		140.79	50.77–60.92	121.0794	0.86	90.63924	Medium
		135.84	50.95–61.14	120.8976	0.89	90.06844	Medium
		126.23	51.13–61.35	121.1808	0.96	89.90424	Medium
		168.22	61.56–73.87	262.4243	1.56	298.6242	Light
		181.13	61.56–73.87	262.6385	1.45	299.27567	Light
		164.40	61.56–73.87	263.04	1.60	300.46188	Light
		143.38	61.56–73.87	262.3854	1.83	298.56501	Light
		118.95	61.56–73.87	262.8795	2.21	270.04226	Medium
		156.28	61.56–73.87	262.5504	1.68	299.00908	Light
154.94	61.5–73.87	263.398	1.70	301.53136	Light		
108.54	63.1–75.82	262.6668	2.42	259.28169	Medium		
147.77	63.1–75.82	263.0306	1.78	288.62422	Light		
84.98	63.1–75.82	262.5882	3.09	259.09954	Medium		
92.48	63.1–75.82	262.6432	2.84	259.21337	Medium		
Ertan Hydropower Station	13	220	26	90	0.41	64.43787	Light
Taiping	9	165	31.3	62.6	0.38	13.91111	Light
Lubuge	8	150	17	34	0.23	28.58766	No
Zhongtianshan Tunnel	8.8	85	10.89	28.37	0.334	17.82243	Light
		90	13.93	29.98	0.333	10.34665	Light
		95	24.88	52.82	0.556	65.69565	Medium
		100	15.04	33.90	0.339	12.59673	Light
		70	9.95	24.51	0.350	12.02266	Light
Baziling Tunnel	6.56	64.6	14.46	31.2	0.483	63.26182	Medium
Shuangjiangkou Hydropower Station	14.94	71.97	15.98	44.80	0.622	41.09527	Light
		77.67	22.11	60.47	0.779	22.96892	Light
		91.47	19.21	52.06	0.569	19.34037	Light
		86.80	37.82	105.25	1.21	91.66741	Medium
		100.6	23.05	64.75	0.636	26.20144	Light
		97.97	32.91	82.32	0.840	74.83285	Medium
Monkey Mountain	12.28	100	28.33	71.73	0.72	77.21841	Medium
Qinling Tunnel	11.2	120	16.6	42.7	0.356	16.90421	Light
			21.9	53.9	0.450	70.72232	Medium
			28.7	68.5	0.570	74.05939	Medium
			22.1	53.16	0.443	19.11458	Light
Micangshan Tunnel	7.1	130	22.78	45.56	0.350	12.8338	Light
Norwegian Xima	31.92	180	48.8	126.9	0.705	19.88597	Light

Table 2 (continued)

Tunnel name	Tunnel diameter D_0/m	σ_{ci}/MPa	σ_1/MPa	$\sigma_{\theta_{max}}/MPa$	$\sigma_{\theta_{max}}/\sigma_{ci}$	$TSGC/MPa \cdot m^{-1}$	Rockburst level
Sweden Headrace	9.24	200	28.0	76–82	0.38–0.41	45.8256	Light
South Africa Hoist Tunnel Room	8.5	198–230	44.3	93.9	0.41–0.47	28.7024	Light
Norwegian Eikesdal Tunnel	6.77	200	30.6	70.6	0.353	36.87414	Light
Japan Guanyue Tunnel	10.4	236	89.0	250.8	1.063	15.558	Light
Norway Sewage Tunnel	2.98	180	35.0	101.5	0.564	22.31	Light
Tianshengqiao Diversion Tunnel	9.58–10.83	115	31.2	78.5	0.683	87.53028	Medium
Jinping Geological Exploration Tunnel	3.39	105–160	25.6	61.7	0.386–0.588	73.72661	Light
Taipingfeng Hydraulic Tunnel	10.25	190–200	30.7	81.9	0.410–0.431	42.65801	Light
Erlang Mountain Highway Tunnel	8.42	56.76	14.84	37.17	0.26	19.96932	Light
		77	40.12	105.92	1.376	115.41879	Medium
		64.9	41.26	41.536	0.64	14.63406	Light
		185.9	20.62	52.06	0.280	28.58766	No
		60.06	28.59	28.829	0.48	10.1285	Light
		92.4	65.96	65.604	0.71	5.858	Violent
		74.14	3.37	8.29	0.11	4.23332	No
		60.5	2.75	7.34	0.12	4.65981	No
		87.12	3.96	8.90	0.10	3.42193	No
		87.12	3.96	7.26	0.08	1.00594	No
		56.76	2.58	14.84	0.26	36.58834	No
		185.9	8.45	20.62	0.11	10.28841	No
		92.4	9.23	25.59	0.277	17.81698	No
Jinping I Hydropower Station	10.92	70.0	35.00	70.00	1.00	12.82051	Light
Yuzixi Diversion Tunnel	6.2	170.0	45.00	90.00	0.529	29.03226	Light
Dongguashan Copper Mine	13.823	132.2	34.3	105.50	0.798	106.31812	Medium
Daxiangling Tunnel	12	59.7	20.8	25.7	0.43	4.08586	No
		114	27.1	55.6	0.488	60.46347	Medium
		123	27.0	56.9	0.463	62.02978	Medium
		132	26.7	62.1	0.47	68.78118	Medium
		116	26.7	29.7	0.256	6.03455	Light
		94	26.6	29.1	0.31	6.13543	Light
		90	25.9	27.8	0.31	6.10026	No
	88	24.1	30.3	0.344	4.32707	Light	

intensities of the engineering examples were classified according to the scale and damage scope. They can be represented in a two-dimensional plane determined by the $TSGC$ and the R , as illustrated in Fig. 4.

According to the existing rockburst criterion based on the strength theory, it is generally believed that the rockburst intensity increases with the increase of the stress–strength ratio R . It can be clearly seen from Fig. 4 that there is no linear relationship between rockburst intensity and $TSGC$ or R . However, in the plane composed of the $TSGC$ and the R , the cases with the same intensity have obvious characteristics of clustering zoning.

Establishment of rockburst criterion

According to the distribution law of the cases in R - $TSGC$ plane, the cases with the same degree of rockburst intensity are divided by horizontal and vertical lines, and Fig. 5 can be obtained.

It can be seen from the Fig. 5 that, when $R \leq 0.2$, no rock burst occurs; in the 5 horizontal sections, the rockburst intensity in the same $TSGC$ horizontal section increases with the increase of R ; in different horizontal sections of $TSGC$, the R threshold of rockburst intensity classification is different. In general, with the increase of $TSGC$, the R threshold of

Fig. 4 Two-dimensional plane determined by the *TSGC* and the *R*

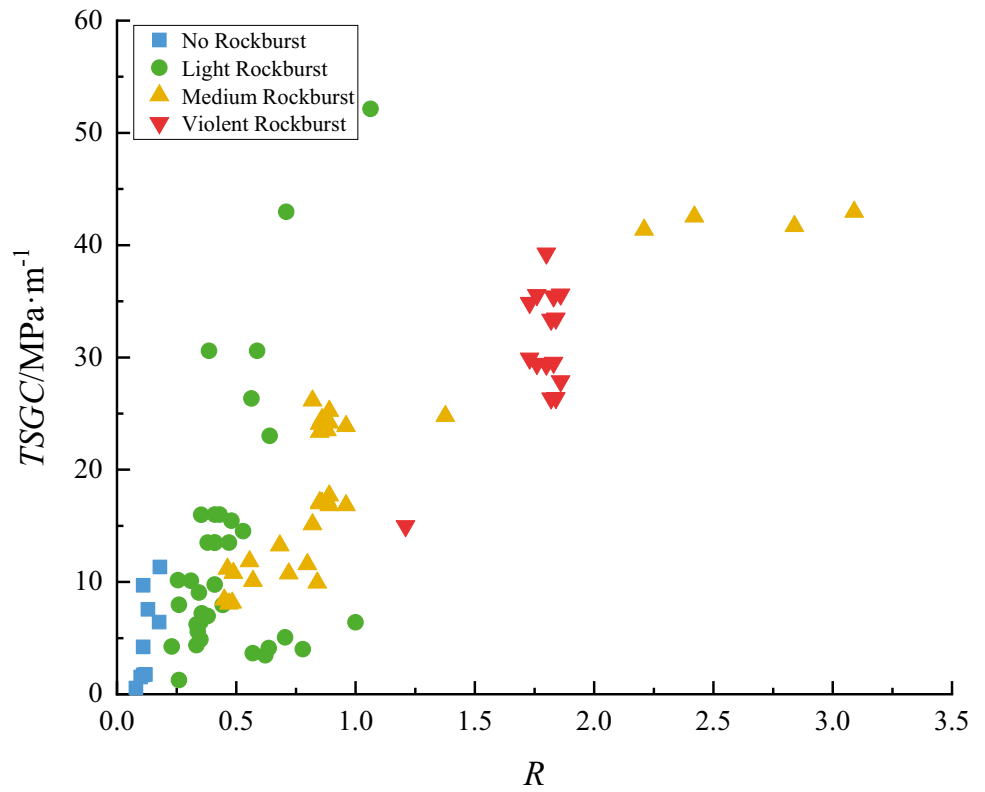


Fig. 5 Fitting map of the rockburst grade areas

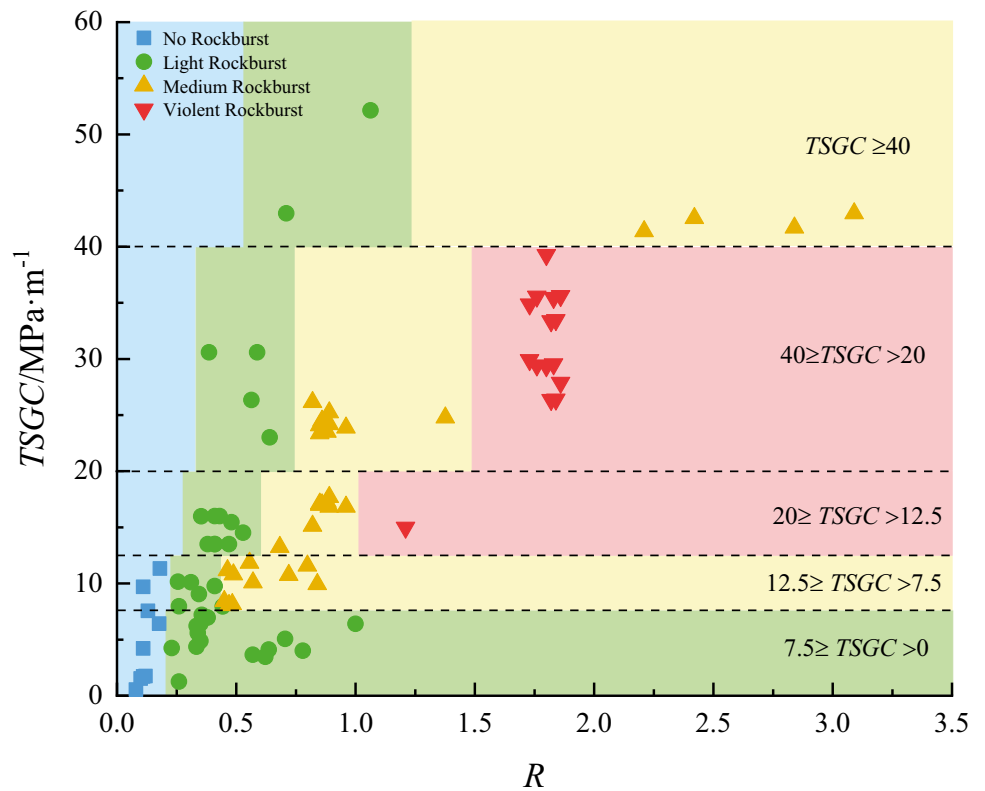


Table 3 Rockburst criterion of SR-SG

Criterion	TSGC/MPa·m ⁻¹	Rockburst intensity			
		No	Light	Medium	Violent
SR-SG	0–7.5	0.20 > R	R ≥ 0.2	—	—
	7.5–12.5	0.22 > R	0.44 > R ≥ 0.22	R ≥ 0.44	—
	12.5–20	0.28 > R	0.60 > R ≥ 0.28	0.97 > R ≥ 0.60	R ≥ 0.97
	20–40	0.33 > R	0.74 > R ≥ 0.28	1.50 > R ≥ 0.74	R ≥ 1.50
	> 40	0.40 > R	2.0 > R ≥ 0.40	R ≥ 2.0	—

rockburst intensity classification increases. The strong rockburst almost occurs in the region where $R \geq 1$ and $TSGC$ is between 13 and 40 MPa·m⁻¹. Based on the partitioning in Fig. 5, the rockburst criterion of SR-SG can be established to determine the rockburst intensity of surrounding rock, as shown in Table 3.

As can be seen from Fig. 5 and Table 3 that the main difference of SR-SG rockburst criterion compared to the traditional rockburst criteria based on strength theory is that, with the increase of $TSGC$, the R threshold of rockburst intensity classification increases. The reason is that when R is the same, the increase of $TSGC$ value means that the tunnel diameter decreases (Eq. (7)). Martin et al. (1999) points out, with the decrease of the hole diameter, the size effect and structure effect of the strength of the surrounding rock become more and more obvious, which makes the stress value for the failure of the inner wall of the tunnel increase significantly, leading to the corresponding increase of the bearing capacity of the surrounding rock.

Analysis of the prediction effects of SR-SG

Comparative analysis of the rockburst case predictions

A comparison was made of the accuracy of the rockburst intensity predictions obtained with the different rockburst criteria according to the statistical data shown in Table 2. The results are shown in Table 4. The predictions of the traditional rockburst criteria based on strength theory are found to have an accuracy of no more than 50%, whereas the prediction accuracy of the SR-SG in this study, which had

Table 4 Comparison of the prediction accuracy of the relevant rockburst criteria

Criterion	SR-SG criterion	Russense criterion	Turchaninov criterion	Hoek criterion	Xu
Prediction accuracy	94.01%	29.27%	47.56%	41.46%	45.12%

considered the stress gradient, was determined to be more than 90%. These results indicated that the proposed criterion is more applicable to rockburst prediction.

Rockburst predictions of the Bayu Tunnel in the Lalin Railway

The Bayu Tunnel is located in the lower reaches of the Sanga section of the southern Tibetan Valley in China. The ground elevations of the tunnel are a range between 3260 and 5500 m, and accordingly, the height difference is about 2300 m. The study area is considered to be a typical alpine valley landform. The mileage of the tunnel is between DK190 + 388 and DK203 + 461. The total length is 1307 m; the maximum buried depth of the tunnel is approximately 2080 m; and the equivalent diameter of the excavation section is 9 m. The lithology of the rock in the study area is singular, and the majority is composed of tertiary medium-angled hornblende black cloud granite. The surrounding rock masses of the tunnel area are relatively complete and mainly composed of types II and III surrounding rock masses, storing high amounts of elastic strain energy. The parameters of the surrounding rock masses are shown in Table 5. It can be seen from the tunnel depth and the parameters of the surrounding rock masses of the project area that the Bayu Tunnel has high-stress field conditions and the lithological conditions which are appropriate for rockburst phenomena to occur.

On October 6 of 2015, the Bayu Tunnel had suffered a rockburst event. As of November 30, 2018, rockburst had frequently occurred during construction activities in the Bayu Tunnel. According to the statistical data, the cumulative length of the rockburst had reached up to 12,111 m. This included 5636 m for the light rockburst, 4944 m for the medium rockburst, and 1531 m for the violent rockburst. These rockburst phenomena had seriously affected the safety

Table 5 The parameters of the surrounding rock masses of the tunnel excavation area

Lithology	σ_{ci} /MPa	σ_t /MPa	Integrity factor K_v
Granite	120	7.6	5.0 to 7.5

Table 6 Rockburst situation and prediction results of the Bayu Tunnel of the Lalin Railway





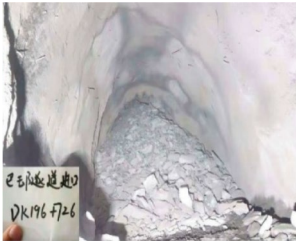





Rockburst location	Destruction phenomenon and rockburst intensities	Rockburst damage patterns at the project site	Stress	Prediction of SR-SG	Prediction of Table 1 method
DK193+566	On September 11, 2016, the vault collapsed in a large area, and a blasting pit with a length of 8 m, maximum depth of approximately 3 m, and a circumferential direction of approximately 7 m was formed (Medium rockburst).		$\sigma_1 = 31$ $\sigma_2 = 20.6$ $\sigma_3 = 7.63$ $\sigma_{\theta\max} = 73.6$ $R = 0.613$ $TSGC = 16.3$	Medium rockburst	Violent rockburst
DK201+520	On July 26, 2017, an “explosive” rockburst occurred in the middle and lower parts of the face. The right side wall formed an irregular curved blasting pit with a length of 5.0 m; a depth of approximately 2.0 m; and a height of approximately 3.0 m. (Light rockburst)		$\sigma_1 = 27.5$ $\sigma_2 = 10.5$ $\sigma_3 = 10.5$ $\sigma_{\theta\max} = 71.2$ $R = 0.59$ $TSGC = 12.73$	Light rockburst	Light or medium rockburst
DK201+410 to DK201+402	On August 29, 2017, a rockburst lasting for 45 hours had occurred, which had caused cracks behind the tunnel face within 60 m. Also, debris was peeled off in large areas, causing a local blasting pit. (Light rockburst)		$\sigma_1 = 29$ $\sigma_2 = 10$ $\sigma_3 = 10$ $\sigma_{\theta\max} = 60.5$ $R = 0.504$ $TSGC = 13.9$	Light rockburst	Medium rockburst
DK195+443	On November 20, 2017, a rockburst occurred on the left side of the tunnel face for approximately 3 m. The rockburst event lasted for more than 90 hours. An irregular blasting pit had formed, with a longitudinal length of approximately 8 m, and a maximum depth of approximately 7 m. (Medium rockburst)		$\sigma_1 = 43$ $\sigma_2 = 22.9$ $\sigma_3 = 7.2$ $\sigma_{\theta\max} = 95.4$ $R = 0.796$ $TSGC = 24.03$	Medium rockburst	Medium or Violent rockburst
DK196+726	On November 15, 2018, a strong rockburst had occurred in the vault in the range of approximately 6 m in the DK196+726 section, which lasted for 50 hours. The rockburst caused a large collapse of the vault. (Violent rockburst)		$\sigma_1 = 42.45$ $\sigma_2 = 22.8$ $\sigma_3 = 8.76$ $\sigma_{\theta\max} = 93.8$ $R = 0.988$ $\eta = 4.67$	Violent rockburst	Violent rockburst

Table 6 (continued)

DK193+545	<p>On September 6, 2016, a rockburst event had suddenly occurred on the right side of the DK190+545, which had rapidly expanded into the deeper part of the surrounding rock masses to form a large-scale wedge-shaped cavity with an influence depth of 3 m.</p> <p>(Violent rockburst)</p>		$\sigma_1 = 31.2$ $\sigma_2 = 20.4$ $\sigma_3 = 7.63$ $\sigma_{\theta\max} = 73.4$ $R = 0.459$ $\eta = 3.84$	Violent rockburst	Light or Medium rockburst
DK194+637	<p>On May 11, 2017, on the left side of the DK194+637, a rock-blast had occurred accompanied with a squeaking sound and a crisp popping sound. The rock mass was lenticular, ribbed, and was ejected out. A wedge-shaped cavity with a depth of approximately 1.5 m was formed.</p> <p>(Medium rockburst)</p>		$\sigma_1 = 40.4$ $\sigma_2 = 22.4$ $\sigma_3 = 7.1$ $\sigma_{\theta\max} = 89.4$ $R = 0.745$ $TSGC = 24.73$	Medium rockburst	Violent rockburst
DK200+091	<p>On December 2, 2017, on the right side of the DK200+091 section, a large number of rock plates were burst off or ejected, and the blasting pit was a pan-shaped cavity with an influence depth greater than 0.5 m.</p> <p>(Light rockburst)</p>		$\sigma_1 = 38.1$ $\sigma_2 = 14.1$ $\sigma_3 = 9.6$ $\sigma_{\theta\max} = 78.08$ $R = 0.65$ $TSGC = 21.87$	Light rockburst	Medium or Violent rockburst
DK193+955	<p>On December 11, 2016, at the vault of DK193+955, a large piece of the surrounding rock masses had continuously burst, and a large volume of rock had appeared to be ejected, forming a “V” shaped shear rock blasting pit.</p> <p>(Medium rockburst)</p>		$\sigma_1 = 34.8$ $\sigma_2 = 21.3$ $\sigma_3 = 7.4$ $\sigma_{\theta\max} = 97$ $R = 0.8$ $TSGC = 20.66$	Medium rockburst	Violent rockburst
DK202+569	<p>On May 11, 2017, a rockburst event occurred on the left side of the DK202+569, in which some of the surrounding rock masses had been loosened and peeled off. The destruction was dominated by cracking, with fresh shell-like failures of the surface areas observed.</p> <p>(Light rockburst).</p>		$\sigma_1 = 26$ $\sigma_2 = 11.2$ $\sigma_3 = 11.2$ $\sigma_{\theta\max} = 66.8$ $R = 0.56$ $TSGC = 12.6$	Light rockburst	Violent or Medium rockburst

and progress of the tunnel construction. The rockburst characteristics and prediction results of the typical rockburst sections are detailed in Table 6.

As can be seen from the prediction results shown in Table 6, the prediction results of each traditional rockburst criterion based on strength theory are quite different, and the overall prediction accuracy of these rockburst criteria was low, which was due to the inconsistent division of the rockburst intensity intervals. However, the early predictions of the rockburst for the Bayu Tunnel are consistent with the actual intensities when the rockburst criterion proposed in this study was based on SR-SG. Therefore, the results had indicated that the proposed criterion is applicable for the predictions of rockburst phenomena.

Conclusions

In this study, based on the analysis results of the main influencing factors of rockburst, the concept of stress gradient was introduced, and a simplified calculation method was proposed. A large number of rock burst engineering examples were used to establish an empirical two-parameter rockburst criterion that comprehensively considered the stress–strength ratio and stress gradient. Main findings are as follows:

1. The concept of stress gradient was proposed to describe the concentration levels of the tangential secondary stress of the surrounding rock masses. The physical meaning was as follows: Change rate of tangential stress on wall of surrounding rock. In terms of its definition, the stress gradient was mainly related to the initial in situ stress, lateral pressure coefficient, and tunnel diameter.
2. It was determined from the statistical analysis results of the engineering rockburst examples that the rockburst intensities were related to the stress magnitudes and stress gradient. The different rockburst intensities had displayed apparent intervals in the two-dimensional plane, which had been determined by the stress gradient and the stress–strength ratio. The prediction accuracy of the empirical relationship of rockburst criterion established in this study which was based on strength theory and had considered the stress gradient had reached more than 90%. Therefore, it had displayed good adaptability potential for actual rockburst predictions in underground projects.
3. The rockburst criterion proposed in this study overcame the problems related to the non-uniformity of the indicator intervals of traditional rockburst criteria based on strength theory. Meanwhile, since the stress concentration is related to the tunnel diameter, the proposed criterion is of great guiding significance for future underground engineering designs, construction projects, and indoor rockburst simulation experiments.

There was observed to be a clear correlation between the rockburst phenomena and the stress gradient. However, due to the limited number of collected rockburst examples in this study, the boundaries of the proposed rockburst criterion could not be accurately classified. Therefore, a large number of engineering examples will still be needed to further improve the proposed rockburst criterion.

Funding The authors acknowledge the financial support provided by the National Natural Science Foundation of China (Grant No. 42002275), the National Natural Science Foundation of Zhejiang province (Grant No. LQ21D020001), the Hubei Key Laboratory of Roadway Bridge and Structure Engineering (Wuhan University of Technology) (No. DQJJ202104), and the Collaborative Innovation Center for Prevention and Control of Mountain Geological Hazards of Zhejiang Province (No. PCMGH-2021–03).

Data availability The data that support the findings of this study are available from the corresponding author upon reasonable request.

Declarations

Conflict of interest The authors declare no competing interests.

References

- Afraei S, Shahriar K, Madani SH (2018) Statistical assessment of rock burst potential and contributions of considered predictor variables in the task. *Tun Under Sp Tech* 72:250–271. <https://doi.org/10.1016/j.tust.2017.10.009>
- Billington D, Estivill-Castro V, Hexel R, Rock A (2011) Requirements engineering via non-monotonic logics and state diagrams. *International Conference on Evaluation of Novel Approaches to Software Engineering* 230:121–135. Springer, Berlin, Heidelberg. https://doi.org/10.1007/978-3-642-23391-3_9
- Diederichs MS (2018) Early assessment of dynamic rupture hazard for rockburst risk management in deep tunnel projects. *J S Afr I Mini Metall* 118(3):193–204. <https://doi.org/10.17159/2411-9717/2018/v118n3a1>
- Dong J, Wesseloo J, Potvin Y, Li X (2016) Discrimination of mine seismic events and blasts using the Fisher classifier, naive Bayesian classifier and logistic regression. *Rock Mech Rock Eng* 49(1):183–211. <https://doi.org/10.1007/s00603-015-0733-y>
- Eberhard E (2001) Numerical modelling of three-dimension stress rotation ahead of an advancing tunnel face. *Int J Rock Mech Min* 38(4):499–518. [https://doi.org/10.1016/S1365-1609\(01\)00017-X](https://doi.org/10.1016/S1365-1609(01)00017-X)
- Feng XT, Xiao YX, Feng GL, Yao ZB, Chen BR, Yang CX, Su GS (2019) Study on the development process of rockbursts. *Chin J Rock Mech Eng* 38(4):649–673. <https://doi.org/10.13722/j.cnki.jrme.2019.0103>
- Forbes B, Vlachopoulos N, Diederichs MS, Hyett AJ, Punkkinen A (2020) An in situ monitoring campaign of a hard rock pillar at great depth within a Canadian mine. *J Rock Mech Geotech* 12(3):427–448. <https://doi.org/10.1016/j.jrmge.2019.07.018>
- Guo WY, Zhao TB, Tan YL, Yu FH, Hu SC, Yang FQ (2017) Progressive mitigation method of rock bursts under complicated geological conditions. *Int J Rock Mech Min* 96:11–22. <https://doi.org/10.1016/j.ijrmms.2017.04.011>
- Hauquin T, Gunzburger Y, Deck O (2018) Predicting pillar burst by an explicit modelling of kinetic energy. *Int J Rock Mech Min* 107:159–171. <https://doi.org/10.1016/j.ijrmms.2018.05.004>

- Huo M, Xia Y, Liu X, Lin M, Wang Z, Zhu W (2020) Evolution characteristics of temperature fields of rockburst samples under different stress gradients. *Infrared Phys Techn* 109:103425. <https://doi.org/10.1016/j.infrared.2020.103425>
- Kaiser PK, Moss A (2022) Deformation-based support design for highly stressed ground with a focus on rockburst damage mitigation. *J Rock Mech Geotech* 14(1):50–66. <https://doi.org/10.1016/j.jrmge.2021.05.007>
- Kong DZ, Cheng Z, Zheng S (2019) Study on the failure mechanism and stability control measures in a large-cutting-height coal mining face with a deep-buried seam. *B Eng Geol Environ* 78(8):6143–6157. <https://doi.org/10.1007/s10064-019-01523-0>
- Li N, Feng X, Jimenez R (2017a) Predicting rock burst hazard with incomplete data using Bayesian networks. *Tunn Under Sp Tech* 61:61–70. <https://doi.org/10.1016/j.tust.2016.09.010>
- Li T, Ma C, Zhu L, Meng L, Chen G (2017b) Geomechanical types and mechanical analyses of rockbursts. *Eng Geol* 222:72–83. <https://doi.org/10.1016/j.enggeo.2017.03.011>
- Li T, Li Y, Yang X (2017c) Rock burst prediction based on genetic algorithms and extreme learning machine. *J Cent South Univ* 24(9):2105–2113. <https://doi.org/10.1007/s11771-017-3619-1>
- Li X, Gong F, Tao M, Dong L, Du K, Ma C, Zhou Z, Yin T (2017d) Failure mechanism and coupled static-dynamic loading theory in deep hard rock mining: a review. *J Rock Mech Geotech Eng* 9(4):767–782. <https://doi.org/10.1016/j.jrmge.2017.04.004>
- Liu N, Zhang CS, Chu WJ, Ni SH (2017) Discussion on the size effect of rock burst risk in deep tunnel. *Chin J Rock Mech Eng* 36(10):2514–2521. <https://doi.org/10.13722/j.cnki.jrme.2017.0326>
- Liu X, Xia Y, Lin M, Wang G, Wang D (2021) Experimental study on the influence of tangential stress gradient on the energy evolution of strainburst. *B Eng Geol Environ* 80(06):4515–4528. <https://doi.org/10.1007/s10064-021-02244-z>
- Luo Y, Wang G, Li X, Liu T, Mandal AK, Xu M, Xu K (2020) Analysis of energy dissipation and crack evolution law of sandstone under impact load. *Int J Rock Mech Min* 132:104359. <https://doi.org/10.1016/j.ijrmms.2020.104359>
- Martin CD, Kaiser PK, McCreath DR (1999) Hoek-Brown parameters for predicting the depth of brittle failure around tunnels. *Can Geotech J* 36(1):136–151. <https://doi.org/10.1139/T98-072>
- Miao SJ, Cai MF, Guo QF, Huang ZJ (2016) Rock burst prediction based on in-situ stress and energy accumulation theory. *Int J Rock Mech Min* 83:86–94. <https://doi.org/10.1016/j.ijrmms.2016.01.001>
- Niu W, Feng XT, Feng G, Xiao Y, Yao Z, Zhang W, Hu L (2022) Selection and characterization of microseismic information about rock mass failure for rockburst warning in a deep tunnel. *Eng Fail Anal* 131:105910. <https://doi.org/10.1016/j.engfailanal.2021.105910>
- Oge IF, Cirak M (2019) Relating rock mass properties with Lugeon value using multiple regression and nonlinear tools in an underground mine site. *B Eng Geol Environ* 78(2):1113–1126. <https://doi.org/10.1007/s10064-017-1179-0>
- Rudziński Ł, Mirek K, Mirek J (2019) Rapid ground deformation corresponding to a mining-induced seismic event followed by a massive collapse. *Nat Hazards* 96(1):461–471. <https://doi.org/10.1007/s11069-018-3552-0>
- Song L, Wang G, Wang X, Huang M, Xu K, Han G, Liu G (2022) The influence of joint inclination and opening width on fracture characteristics of granite under triaxial compression. *Int J Geomech* 22(5):04022031. [https://doi.org/10.1061/\(ASCE\)GM.1943-5622.0002372](https://doi.org/10.1061/(ASCE)GM.1943-5622.0002372)
- Taromi M, Eftekhari A, Hamidi JK, Aalianvari A (2017) A discrepancy between observed and predicted NATM tunnel behaviors and updating: a case study of the Sabzkuh tunnel. *B Eng Geol Environ* 76(2):713–729. <https://doi.org/10.1007/s10064-016-0862-x>
- Wang C, Wu A, Lu H, Bao T, Liu X (2015) Predicting rockburst tendency based on fuzzy matter-element model. *Int J Rock Mech Min* 75:224–232. <https://doi.org/10.1016/j.ijrmms.2015.02.004>
- Wojtecki Ł, Iwaszenko S, Apel DB, Bukowska M, Makówka J (2022) Use of machine learning algorithms to assess the state of rockburst hazard in underground coal mine openings. *J Rock Mech Geotech* 14(3):703–713. <https://doi.org/10.1016/j.jrmge.2021.10.011>
- Xie H, Gao F, Ju Y (2015) Research and exploration of deep rock mechanics. *Chin J Rock Mech Eng* 34(11):2161–2178. <https://doi.org/10.13722/j.cnki.jrme.2015.1369>
- Yu H, Wang Q (2021) Analytical solution for deep circular tunnels covered by an isolation coating layer subjected to far-field shear stresses. *Tunn Undergr Sp Tech* 115:104026. <https://doi.org/10.1016/j.tust.2021.104026>
- Zhao G, Wang D, Gao B, Wang S (2016) Modifying rock burst criteria based on observations in a division tunnel. *Eng Geol* 216:153–160. <https://doi.org/10.1016/j.enggeo.2016.11.014>
- Zhou J, Li X, Shi X (2012) Long-term prediction model of rockburst in underground openings using heuristic algorithms and support vector machines. *Safety Sci* 50(4):629–644. <https://doi.org/10.1016/j.ssci.2011.08.065>

Springer Nature or its licensor (e.g. a society or other partner) holds exclusive rights to this article under a publishing agreement with the author(s) or other rightsholder(s); author self-archiving of the accepted manuscript version of this article is solely governed by the terms of such publishing agreement and applicable law.